

# Site-Selective Oxidative Coupling Reactions for the Attachment of Enzymes to Glass Surfaces through DNA-Directed Immobilization

Kanwal S. Palla,<sup>†,§</sup> Tyler J. Hurlburt,<sup>†,‡,§</sup> Alexander M. Buyanin,<sup>†,⊥</sup> Gabor A. Somorjai,<sup>†,‡,⊥</sup> and Matthew B. Francis<sup>\*,†,⊥</sup>

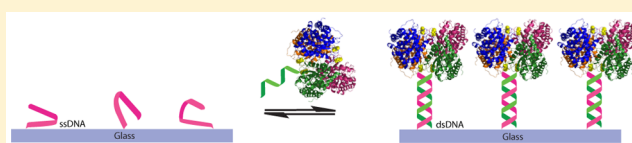
<sup>†</sup>Department of Chemistry, University of California, Berkeley, California 94720-1460, United States,

<sup>‡</sup>Chemical Sciences Division, Lawrence Berkeley National Laboratories, Berkeley, California 94720-1460, United States, and

<sup>⊥</sup>Materials Sciences Division, Lawrence Berkeley National Laboratories, Berkeley, California 94720-1460, United States

**S** Supporting Information

**ABSTRACT:** Enzymes are able to maintain remarkably high selectivity toward their substrates while still retaining high catalytic rates. By immobilizing enzymes onto surfaces we can heterogenize these biological catalysts, making it practical to study, use, and combine them in an easily controlled system. In this work, we developed a platform that allows for the simple and oriented immobilization of proteins through DNA-directed immobilization. First, we modified a glass surface with single-stranded DNA. We then site-selectively attached the complementary DNA strand to the N-terminus of a protein. Both DNA modifications were carried out using an oxidative coupling strategy, and the DNA strands served as easily tunable and reversible chemical handles to hybridize the protein–DNA conjugates onto the surface. We have used the aldolase enzyme as a model protein to conduct our studies. We characterized each step of the protein immobilization process using fluorescent reporters as well as atomic force microscopy. We also conducted activity assays on the surfaces with DNA-linked aldolase to validate that, despite being modified with DNA and undergoing subsequent immobilization, the enzyme was still able to retain its catalytic activity and the surfaces were reusable in subsequent cycles.



## INTRODUCTION

Traditionally, catalysis research has been undertaken as the three separate disciplines involving homogeneous complexes, heterogeneous structures, and enzymes. As such, the tools to determine mechanistic information have largely evolved separately. In previous work, we have successfully converted homogeneous catalysts into heterogeneous systems, merging high reaction selectivity with the advantages of catalyst recovery,<sup>1</sup> ability to be employed in continuous flow processes,<sup>2</sup> and compatibility with surface-sensitive characterization techniques.<sup>3</sup> To integrate enzymes into heterogeneous systems, there is a need for new immobilization strategies that are site-selective, general, and inherently capable of combining multiple species into complex arrays. With the overall goal of studying the dynamics of enzyme behavior using sum frequency generation vibrational spectroscopy and other techniques suited for heterogeneous systems,<sup>4</sup> we have developed an efficient surface attachment strategy based on DNA hybridization. An interesting feature of this approach is the use of two different reaction modes of a family of oxidative coupling methods, allowing a unified strategy for modifying both the surface and the protein components with pendant nucleic acid groups.

The utility of immobilizing proteins onto a surface spans a variety of applications, including the study of protein–protein interactions, enzyme kinetic studies, biosensors, bioanalytics, and even industrial biocatalytic processes.<sup>5–7</sup> These studies create a constant need for effective and facile ways to assemble

protein microarrays. Many protein immobilization chemistries involve the direct attachment of proteins to surfaces through short linkers and reactive handles. Common approaches include nonspecific covalent modification of native amino acid side chains on the surface of a protein, such as lysine acylation with NHS esters. However, it has been found that randomly oriented proteins can exhibit reduced accessibility of active sites and display lower activities than their ordered counterparts.<sup>7–9</sup>

Because an ordered display of proteins is often more favored, both covalent and non-covalent strategies to orient proteins uniformly on surfaces have been developed. Covalent approaches have taken advantage of maleimide reactivity with thiols,<sup>9</sup> native chemical ligation,<sup>10</sup> photochemical thiol–ene chemistry,<sup>11</sup> carbohydrate moieties,<sup>12</sup> Si-tags,<sup>13</sup> and enzymatic tags,<sup>14,15</sup> to name a few. Representative non-covalent systems are exemplified by polyhistidine tag incorporation via genetic engineering to bind to Ni-NTA-functionalized surfaces, as well as biotin–streptavidin complexation.<sup>16–18</sup> Another non-covalent protein immobilization approach is through the use of DNA, taking advantage of complementary strand hybridization. This type of DNA-directed immobilization (DDI) requires that the surface be functionalized with a short oligonucleotide and that its complementary strand be conjugated to the target

Received: November 12, 2016

Published: December 21, 2016

protein such that the hybridization of the two strands will lead to the controlled immobilization of the proteins under chemically mild and biocompatible conditions. DDI has shown reliability and has been used in tandem with a variety of other assembly processes. It has also been reported that the DDI strategy is an efficient method to immobilize proteins because of the easily adjustable linker it provides, thereby helping to prevent protein denaturation.<sup>19–21</sup>

Previously, protein surfaces have been created with this strategy via the complexation of biotinylated antibodies and biotinylated DNA, brought together with streptavidin, that were then immobilized on streptavidin–biotin DNA-modified surfaces via DNA hybridization.<sup>22</sup> Additionally, clickable functional groups that can bind to native tyrosine residues have been used to create DNA–protein conjugates which were then immobilized on similar streptavidin-based surfaces.<sup>23</sup> Because DNA molecules are highly stable, they can easily undergo chemical modification in preparation for DDI. In another example, a DNA–heme was generated and used to reconstitute two separate heme binding proteins: apo-myoglobin and apo-horseradish peroxidase. These were tethered onto microplates that were coated with the complementary DNA strands, and it was shown that enzymatic activity of both proteins was retained.<sup>24</sup> Even more recently, unnatural amino acid incorporation was used to insert a *p*-acetylphenylalanine residue into a monoclonal antibody, which was then used as a handle for ligation with an aminoxy-functionalized single-stranded DNA.<sup>25</sup> These approaches illustrate both the benefits and the complexities involved in generating protein–DNA bioconjugates.

We have previously developed several site-selective protein modification reactions, and we have shown the applicability of some of them in the synthesis of DNA surfaces and DNA–protein bioconjugates.<sup>26–34</sup> More recently, we reported on an oxidative strategy that is able to couple an *o*-aminophenol (AP) to either an aniline moiety or the N-terminal amino group of peptides and proteins using potassium ferricyanide as the oxidant.<sup>35,36</sup> This reaction involves the intermediacy of an iminoquinone intermediate, to which the aniline or N-terminal amine adds. Following reoxidation of the resulting amino-phenol species, hydrolysis of the iminoquinone imine yields the final ketone group. Aniline addition products prefer the tautomer shown in Figure 1a, path a, while additions with N-terminal prolines sit as the *o*-quinone species shown in Figure 1a, path b. Both type of products are highly stable and resist hydrolysis.

Herein, we take advantage of this positional selectivity and functional group tolerance and apply it toward the development of a DDI-based platform as shown in Figure 1b. We first coupled an *o*-aminophenol-modified DNA strand to an aniline-modified glass surface. Separately, we modified our protein of interest at the N-terminus with a complementary *o*-aminophenol-substituted DNA strand in a single step with low concentrations of reagents. The subsequent hybridization of the surface oligo with the complementary oligo–protein conjugate allowed for the controlled attachment of the protein to surfaces in an oriented and versatile manner. We then apply DNA hybridization-based protein immobilization using aldolase and evaluate its catalytic activity after attachment to glass slides. We also study the reusability and regenerability of these surfaces.

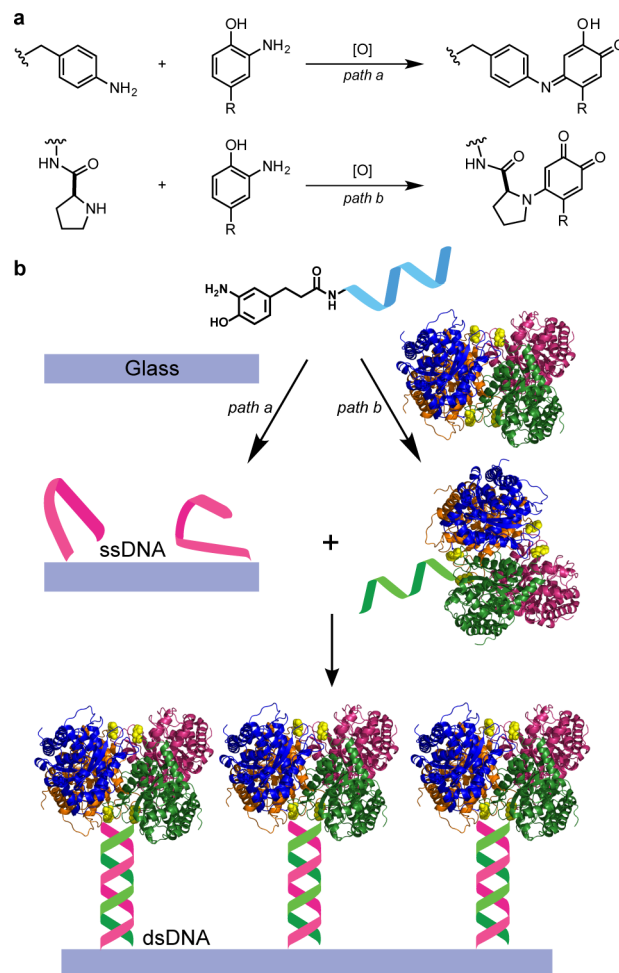


**Figure 1.** DNA-directed immobilization. (a) Reaction pathways for oxidative coupling of an *o*-aminophenol to an aniline moiety and to an N-terminal proline residue. (b) Schematic of DNA directed immobilization of a site-selectively modified DNA–protein conjugate onto a glass surface displaying complementary single-stranded DNA.

## RESULTS AND DISCUSSION

### Modifying Glass Slides with Single-Stranded DNA and Hybridizing to Complementary DNA.

Most previous studies of DDI-based protein immobilization have used gold or coated plastic substrates.<sup>19</sup> For these studies we selected glass slides because of their advantages for spectroscopic and microscopic analysis. We used silanization with 3-(4-azidophenyl)-*N*-(3-trimethoxysilylpropyl) propanamide followed by TCEP reduction in order to derivatize glass with aniline functional groups.<sup>32</sup> We then synthesized the aminophenol-modified strand A (AP-A), a 20 base oligomer (SI Figure S2), and coupled it to the aniline surface in the presence of potassium ferricyanide as an oxidizing agent (Figure 2a). Once the glass slides were modified with AP-A, each surface was incubated with complementary strand, A', which had a fluorophore conjugated to its 5' end (A'\*). Non-complementary AP-B was also synthesized to be used as a negative control for the surface modification. Following hybridization and rinsing, fluorescent images were collected to confirm that the DNA-mediated hybridization between A and A'\* was specific (Figure 2b). Fluorescence intensity on these slides was 50-fold greater than that of the mismatched control between B and A'\* (Figure 2c), indicating that there was only nominal

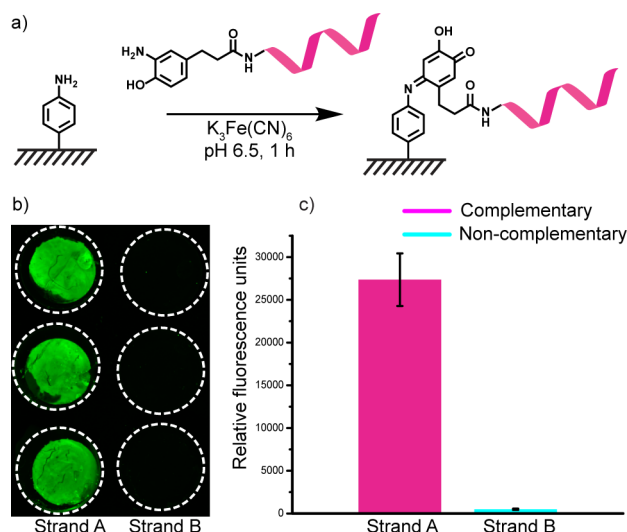


**Figure 2.** Modification of aniline coated glass slides with single-stranded DNA. (a) Schematic of an oxidative coupling reaction for single-stranded DNA attachment to aniline-modified surfaces. (b) Fluorescence studies to verify DNA strand hybridization. After attachment of strand A or strand B, glass slides were incubated with a fluorescently tagged DNA ( $A^*$ ). Fluorescence signal was evaluated when there was sequence complementarity (left column, strands A and  $A^*$ ) and when there was not (right column, strands B and  $A^*$ ). (c) Plot of fluorescence intensities, conducted in triplicate. The fluorescence intensity on the complementary slides was 50-fold greater than on the non-complementary slides.

non-specific binding of  $A^*$  onto the glass surface. The procedure used for surface DNA attachment was optimized (concentration, buffer conditions, time) to give the greatest difference in fluorescence between complementary and non-complementary strands. DNA sequences used in these studies are highlighted in Table 1.

**Modifying Aldolase with  $A'$  DNA and Evaluating Its Activity.** A fructose-bisphosphate aldolase (ALD) from rabbit muscle was chosen as a protein of particular interest for these studies. Aldolase is a protein involved in a series of enzymes within the glycolytic pathway, as it catalyzes the reversible breakdown of fructose-1, 6-bisphosphate (FBP) to glyceraldehyde-3-phosphate (G3P) and dihydroxyacetone phosphate (DHAP) as seen in Figure 3a. Because it is involved in a C–C bond-breaking and (in the microscopic reverse) bond-forming reaction, it is of particular importance in industrial processes that can engineer the enzyme to be promiscuous and catalyze other C–C bond processes.<sup>37</sup> It is a homotetramer with  $D_2$  symmetry (PDB: 6ALD). All four of the N-termini are solvent exposed, with two N-termini in proximity to one another and the other two N-termini on the opposite face. As a result of this configuration, there are two possible ways for the protein to be immobilized via its N-terminal positions.

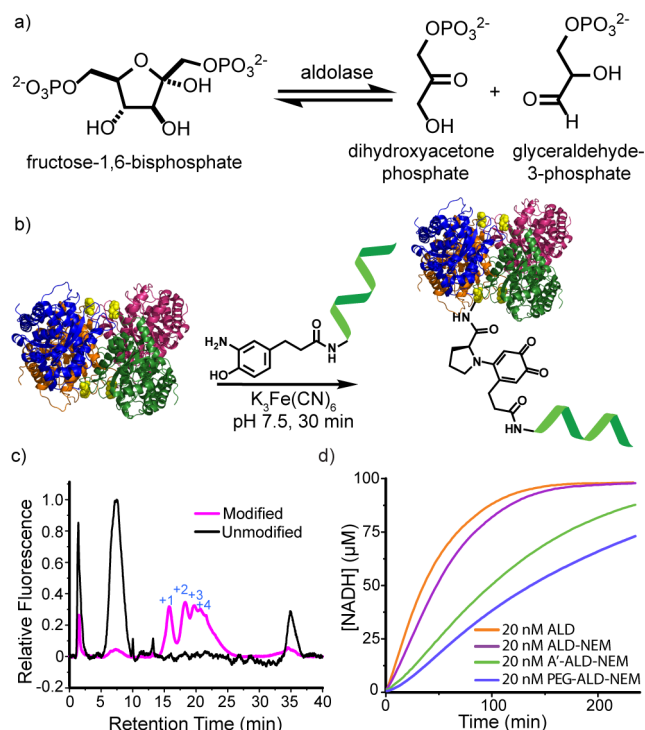


**Figure 3.** Aldolase modification with DNA. (a) Conversion of fructose-1,6-bisphosphate into glyceraldehyde-3-phosphate and dihydroxyacetone-phosphate by aldolase. (b) Schematic of protein modification at the N-termini (yellow) with aminophenol-modified DNA. (c) Anion-exchange HPLC traces of NEM-capped aldolase (black) and NEM-capped aldolase modified with single-stranded DNA (pink) showing multiple modifications. (d) Quantification of solution activity of unmodified aldolase (orange), aldolase with reactive cysteines capped with NEM (purple), and NEM-capped aldolase after modification with  $A'$  DNA (green) and 5 kDa PEG (blue). Samples were analyzed in triplicate, and data points were collected every 2 min. Initial rates were  $1.473 \pm 0.009 \mu\text{M}/\text{min}$  for unmodified aldolase,  $1.030 \pm 0.006 \mu\text{M}/\text{min}$  for NEM-capped aldolase,  $0.499 \pm 0.003 \mu\text{M}/\text{min}$  for NEM-capped aldolase modified with DNA, and  $0.391 \pm 0.002 \mu\text{M}/\text{min}$  for NEM-capped aldolase modified with PEG. All assays were run at  $37^\circ\text{C}$  and conducted in triplicate.

Fortunately, these would be expected to display the protein with highly similar orientations. Additionally, it retains a proline residue at its N-terminus, which has a favorable propensity toward the oxidative coupling reaction.<sup>36</sup>

As the cysteine residues of aldolase are not required for catalytic activity, they were first capped with *N*-ethyl-maleimide (NEM) to prevent participation in the oxidative coupling reaction (SI Figure S3). For future studies involving enzymes that rely on free cysteine groups, we have recently shown that Ellman's reagent (DTNB) can also be used.<sup>38</sup> AP- $A'$  was synthesized and coupled to the aldolase N-terminus using

**Table 1.** DNA Sequence Information

name	sequence	$T_m$ ( $^\circ\text{C}$ )
A	5'-CCC TAG AGT GAG TCG TAT GA-3'	52.6
Ax	5'-CCC TAG AGT GAG TCG TAT GAA AAA A-3'	54.4
$A'$	5'-TCA TAC GAC TCA CTC TAG GG-3'	52.6
$Ax'$	5'-TTT TTT CAT ACG ACT CAC TCT AGG G-3'	54.4
$A^*$	5'-AlexaFluor488 TCA TAC GAC TCA CTC TAG GG-3'	52.6
B	5'-AGT GAC AGC TGG ATC GTT AC-3'	54.4

potassium ferricyanide-mediated oxidative coupling (Figure 3b). Free DNA was removed through spin concentration, and a BCA assay was used to quantify the total protein remaining. Additionally, HPLC with an anion-exchange column and tryptophan fluorescence detection was used to determine the level of modification of the DNA–aldolase bioconjugate. Less than 5% of the total protein was unmodified with DNA, and a range of modifications from one to four DNA strands per tetramer were seen (Figure 3c).

Solution activity assays were carried out on aldolase, aldolase capped with NEM, and NEM-capped aldolase that was modified separately with AP-A' DNA and aminophenol 5 kDa polyethylene glycol (PEG) to determine how the modification itself as well as reaction conditions impacted the enzymatic activity. The 5 kDa PEG modification was chosen because of its comparability to the 20-base A' DNA in molecular weight while having a neutral charge. Glyceraldehyde-3-phosphate dehydrogenase (GAPDH) was paired with aldolase in the activity assays. GAPDH catalyzes the conversion of G3P to 1,3-bisphosphoglycerate in the presence of NAD<sup>+</sup> as a cofactor. The conversion of NAD<sup>+</sup> to NADH can be monitored by the increase in absorbance at 340 nm and can be used to quantify aldolase activity. As illustrated in Figure 3d, NEM-capped aldolase after modification with DNA retained about 48% of its enzymatic activity (PEG-modified aldolase retained 38% of its activity). This difference could be attributed to the DNA (or PEG) sterically hindering accessibility of the active site.

Aldolase capped with DTNB was modified at the N-terminus with a small molecule aminophenol (2-amino-*p*-cresol). After removal of the cysteine cap, the bioconjugate was analyzed by ESI-TOF mass spectrometry and showed high yields of a single *p*-aminocresol addition (SI Figures S4 and S5). A trypsin digestion of this sample confirmed that the modification was occurring at the N-terminal peptide fragment (SI Figure S7) and subsequent MS/MS analysis confirmed that the oxidative coupling-mediated modification was occurring site-selectively at the N-terminal proline residue of aldolase (SI Figure S8).

**Evaluating the Activity of Surface-Immobilized Aldolase.** The A'-aldolase bioconjugate was incubated on A-modified (complementary) surfaces to allow for DNA-directed immobilization. Enzymatic activity was subsequently evaluated and the results of these assays are shown in Figure 4a. Because hybridization to the surface is an internal purification tool, unmodified aldolase did not need to be purified away from DNA-modified aldolase. In order to evaluate any non-specific binding that was occurring, a control was included where the DNA–protein conjugate was incubated on B-modified (non-complementary) surfaces. As compared to the control, we observed that when A'-aldolase was incubated on the surface displaying its complementary strand, aldolase activity was significant, and background activity was minimal. This confirmed that aldolase was successfully immobilized with very low levels of non-specific adsorption and that the surface immobilization itself did not destroy its quaternary structure. An additional control was included with 20 nM free A'-aldolase in solution to ensure that the assay was functioning as expected. This amount of protein represents the theoretical maximum amount that can be on the surface, as determined by dividing the total area of the experimental region by the “footprint” each protein would occupy. Fluorescence studies were also conducted to visualize each step qualitatively, and are depicted in SI Figures S9 and S10.

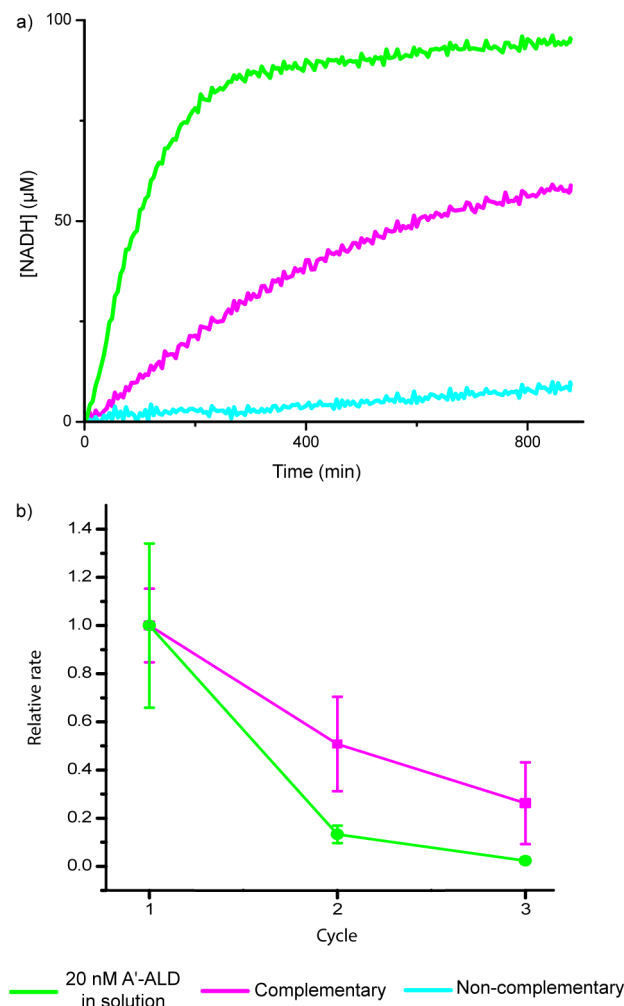


**Figure 4.** Testing the activity of DNA-aldolase conjugates immobilized after hybridization to the glass surface. a) Activity assay of A'-aldolase exposed to a glass surface displaying the complementary DNA strand (A, pink), the non-complementary DNA strand (B, blue), and free in solution at a concentration of 20 nM (green). b) Testing the reusability of surface immobilized aldolase over three 24 h cycles. Activity assays of cycles 2 and 3 are shown in SI Figure S12. All assays were run at 37 °C and conducted in triplicate.

**Reusing the Protein-Immobilized Surfaces.** Given the successful immobilization of aldolase onto the glass slides, we were interested in investigating the reusability of the surfaces. We ran each cycle for 15 h, rinsed reagents from the wells and repeated the assay using the same surface. These data are shown in Figure 4b and SI Figure S12. It can be seen that, while we do see a drop in activity in each subsequent cycle, about half of the activity is maintained from one run to the next. We hypothesized that because the assay was conducted at 37 °C, the temperature could be attributing to inactivation of the protein over time. To test this, we incubated unmodified aldolase in solution at 37 °C for lengths of time equivalent to each iterative cycle, and we observed that the drop in activity was in fact a result of the protein being exposed to the elevated temperatures for extended periods of time (SI Figure S13).

**Surface Characterization with Atomic Force Microscopy.** Atomic force microscopy (AFM) studies were carried out at the various stages of the surface modification process on mica surfaces. Mica was chosen due to its atomically flat nature.<sup>39</sup> This allowed for verification that any changes to the

surface morphology were due solely to the chemistries we applied and not the underlying morphology of the substrate. Additionally, free surface silanol groups on mica allowed for identical surface chemistry to that used on the glass slides. AFM images were taken of surfaces functionalized with (a) aniline, (b) single-stranded DNA (sequence A), (c) double-stranded DNA (sequence A' hybridized to sequence A), and (d) immobilized aldolase via DNA hybridization (A'-aldolase hybridized to A) (Figure 5). It was seen that the aniline-

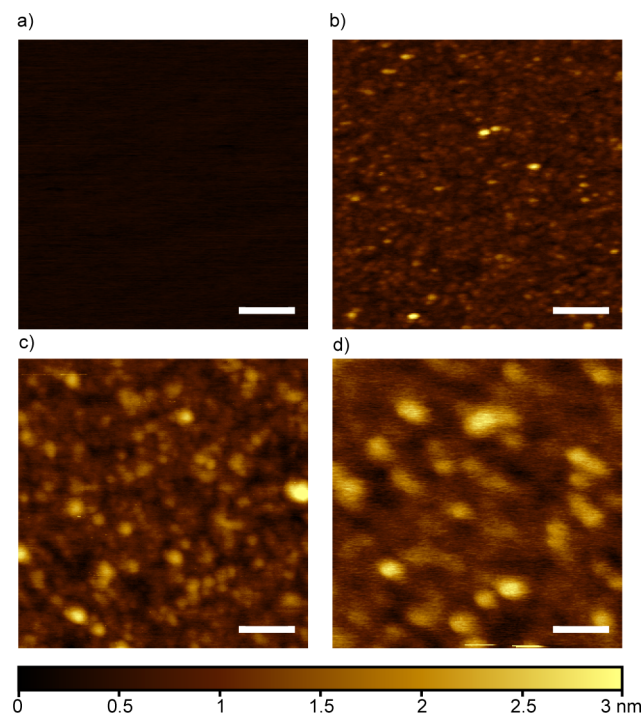


**Figure 5.** Height AFM images taken in non-contact mode of (a) aniline-modified mica, (b) mica functionalized with single-stranded DNA, (c) complementary DNA hybridized to mica functionalized with single-stranded DNA, and (d) complementary DNA–aldolase conjugate hybridized to mica functionalized with single-stranded DNA. Scale bars are 50 nm.

functionalized surface was uniformly flat, showing minimal variation in height over the observed region. Upon the attachment of single-stranded DNA, the surface became rougher, showing a high density of small features of increased height. These features became larger in area upon addition of the complementary strand of DNA. The addition of the A'-aldolase conjugate to a surface displaying single-stranded A DNA continued the trend of increasing morphological heterogeneity. These images verified that the surface was becoming more complex at each stage of the modification process, and thus the morphologies are changing in a manner consistent with what we expected to see based on the fluorescence imaging studies.

**Hybridization Temperature Modulates Immobilization Levels.** Previous reports have suggested that levels of modification on the surface play a significant role in activity levels, and that higher surface coverage does not always correlate to higher activity due to the effects of over-crowding and blockage of enzyme active sites.<sup>40</sup> Given this information, having a method to tune the level of modification in either direction could prove useful for tailoring these surfaces for different proteins. For all of the experiments described thus far,

hybridization between DNA-aldolase and DNA-modified glass surfaces was carried out at room temperature. Interestingly, when hybridization temperatures were varied (4, 23, and 37 °C), it was observed that the increasing temperatures resulted in increasing levels of protein immobilization. This was first determined through backfilling of open ssDNA sites (at 23 °C) after aldolase had been immobilized, where an expected trend of decreasing fluorescence with increasing annealing temperature was observed when the average fluorescence was quantified for the total surface area of the glass slides (Figure 6a,b). We hypothesize that the closer the hybridization temperature is to the melting temperature of the DNA strands (52.6 °C), the more efficient the thermal annealing becomes because the strands can melt and rehybridize to reach optimal

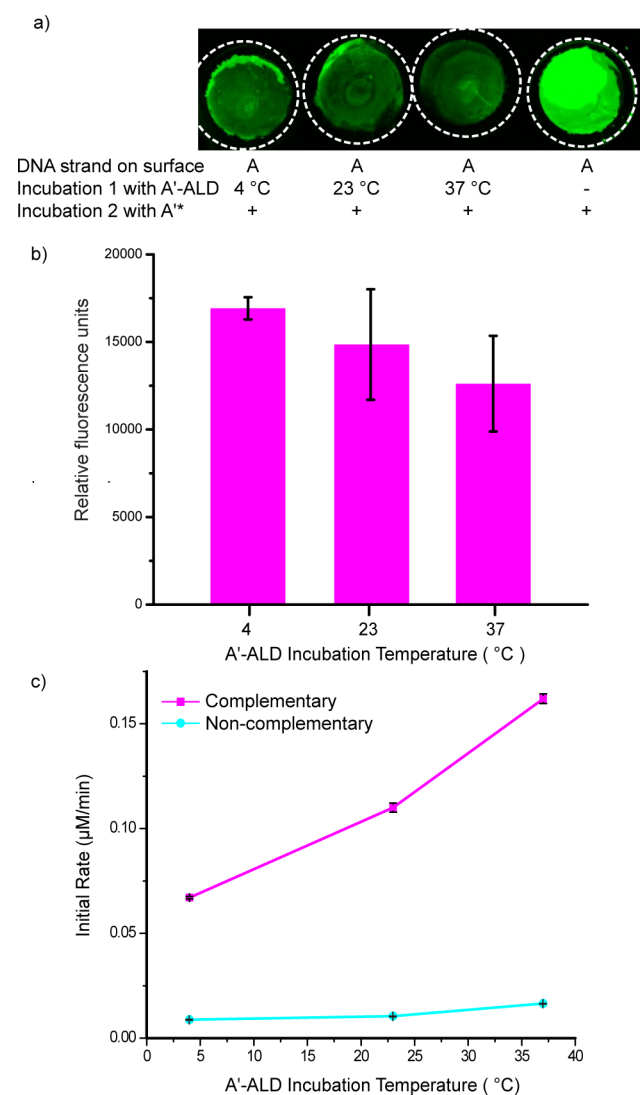


**Figure 6.** Impact of annealing temperature on surface hybridization levels. (a) Fluorescence images of glass slides modified with A, then incubated with A'-aldolase at varying temperatures. Subsequent incubation with fluorescently tagged DNA, A'\*, allowed for backfilling of open surface DNA sites. (b) Quantification of fluorescent slides. Lower fluorescence corresponds to greater hybridization of the A'-aldolase conjugate. (c) Initial rates of A'-aldolase activity when immobilized on surfaces with strand A (complementary) or strand B (non-complementary) at varying incubation temperatures, conducted in triplicate.

coverage. At a lower temperature the strands are more restricted to the first location of hybridization, leading to lower levels of surface coverage. We also observed an increase in aldolase activity at the higher levels of modification, and could use this approach to refine our surfaces further (Figure 6c). Additionally, in the future, we envision using temperature variations to determine the levels at which we can saturate surfaces with enzymes without impeding their catalytic activity, in an effort to obtain surfaces with maximum efficiency.<sup>41</sup>

**Regenerating and Recycling the Single-Stranded DNA-Modified Surfaces.** A particularly noteworthy advantage of using DDI to orient proteins onto solid surfaces is that the DNA strands can be separated in order to remove the DNA-aldolase conjugate and regenerate the surface bearing single-stranded DNA. This allows for storage of the slides for an extended period of time due to the stability of DNA, and ultimately the ability to reuse them in future assays. We used DNA strand displacement to remove the DNA-aldolase conjugate and then rehybridized a fresh batch of DNA-aldolase. In this assay, we conjugated aldolase onto 25 base strand Ax', where 20 bases were complementary to A, but the remaining 5 served as an overhang. Ax'-aldolase was immobilized to glass slides displaying A. Then, Ax, a 25-base strand with complete complementarity to Ax', was used to displace Ax'-aldolase from the surface. This surface was then reused, and a fresh batch of Ax'-aldolase was immobilized. Activity assays of the surfaces at each stage were carried out, and as seen in Figure 7, the activity of aldolase immobilized on fresh glass slides remained consistent with the activity observed on aldolase that was immobilized on a regenerated glass slide. Fluorescence studies also corroborated these trends (SI Figure S14).

The ability to recycle the DNA-modified glass slides will be of particular use for slides with more complex DNA patterns. It should be possible to pattern the glass with multiple different DNA strands with spatial control, creating an ordered array that would selectively bind multiple enzymes, allowing for the catalysis of a complex series of reactions.

## CONCLUSIONS

In this work, we have prepared a single class of aminophenol-substituted DNA strands and used them to modify both glass surfaces and protein N-termini. By piecing together each component, we have developed a step-by-step platform for producing oriented displays of proteins on glass surfaces. We have qualitatively verified our chemistry at each stage through fluorescence studies and AFM, and have also demonstrated its utility by testing the enzymatic activity of surface immobilized aldolase. This allows for the oriented immobilization of proteins with an adjustable spacer, where the enzyme can be reused in multiple cycles. Additionally, through DNA strand displacement, we have successfully regenerated the single-stranded DNA bearing glass surfaces, and we have shown them to be reusable in subsequent hybridization assays. The chemistry involved in attaching the first strand of DNA to the surface is convenient, quick, and stable, and works on inexpensive glass slides. The conjugation of the complementary DNA strands to proteins is biocompatible, quick, and only requires low concentrations of the coupling partners. In addition, because the native N-terminal amine is being targeted as the attachment site, it can be applied to a large scope of proteins with minimal genetic engineering being required, this could include thermostable enzymes which would give longer lifetimes.

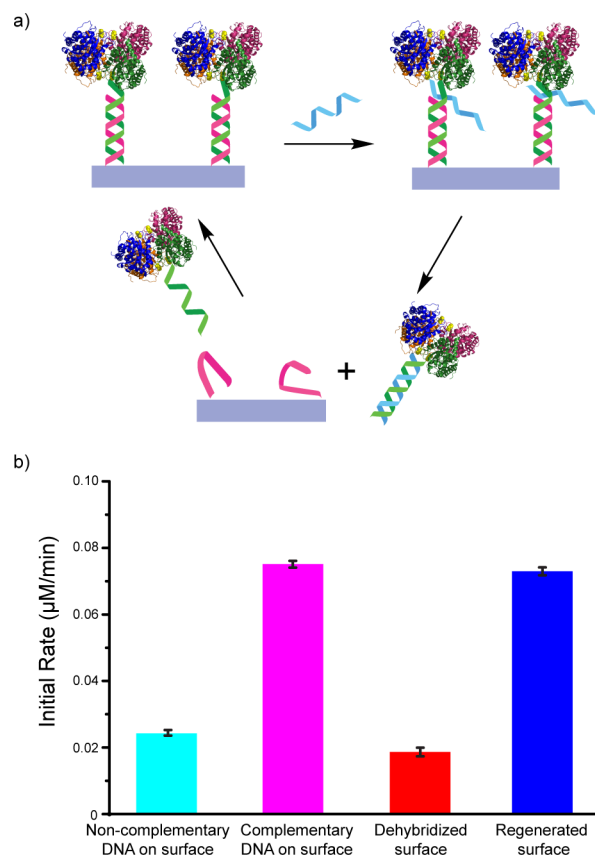


**Figure 7.** Testing the activity of regenerated DNA-aldolase conjugates immobilized on glass surfaces. (a) Schematic of DNA strand displacement-mediated surface regeneration. (b) Initial rates of the activity of Ax'-aldolase exposed to a glass surface displaying the non-complementary DNA strand (strand B), and the complementary DNA strand (strand A) were obtained. Then, DNA strand displacement was carried out to remove the Ax'-aldolase conjugate from the glass surface. The regenerated surfaces were then incubated with a new batch of Ax'-aldolase. Initial rates of activity for both of these surfaces were obtained. All assays were run at 37 °C and conducted in triplicate.

Because we have used DNA hybridization as our mode of protein attachment, the easily accessible diversity of DNA strands offer a wide range of attachment handles, both in terms of linker length and rigidity. Additionally, the generalizable nature of this DDI method should facilitate the immobilization of a variety of proteins. Given all of these advantages provided by this approach, we seek to enhance this platform further in the future.

Taking advantage of the transparent nature of the glass surfaces used in these studies, we are also seeking to characterize these surfaces using alternative spectroscopic techniques, such as sum frequency generation and X-ray photoelectron spectroscopy, to gain information about the orientation and coverage of the protein.<sup>4,42,43</sup>

## EXPERIMENTAL SECTION

**Patterning Single-Stranded DNA on Aniline-Functionalized Slides Using Potassium Ferricyanide-Mediated Oxidative Coupling.** Aniline-functionalized 15 mm circular glass slides were modified with ssDNA. A 4.5 μL drop of 50 μM aminophenol-modified DNA, 1 mM K<sub>3</sub>Fe(CN)<sub>6</sub> and 250 mM NaCl in 10 mM pH 6.5 phosphate buffer was placed on the center of the aniline glass slide. Another unmodified glass slide was placed on top of the drop causing

the DNA solution to spread over the slide in a sandwich. Slides were allowed to sit in the dark at RT for 1 h. Then, slides were dipped in water and the unmodified glass slides were removed from the DNA-modified glass. DNA-modified glass slides were rinsed in 0.4% SDS and then 10 mM pH 6.5 PBS each at RT for 5 min with stirring. Slides were rinsed in Nanopure water and dried with a stream of N<sub>2</sub>. The single-stranded DNA displaying glass slides were stored at RT in a desiccator until use.

**Synthesis of Aldolase–DNA Bioconjugate.** To aldolase (20  $\mu$ M) in 10 mM phosphate buffer, pH 7.5 was added 5 equiv of the *o*-aminophenol-modified DNA (100  $\mu$ M). The solution was briefly vortexed, and then 10 equiv (relative to the *o*-aminophenol) of K<sub>3</sub>Fe(CN)<sub>6</sub> (as a 10 mM solution in 10 mM phosphate buffer, pH 7.5) was added. After 30 min, the reaction was purified by repeated (>12 times) centrifugal filtration against a 30 kDa MWCO membrane (Millipore), allowing for purification of aldolase and aldolase-DNA conjugate from free DNA. Modification was monitored by a combination of SDS-PAGE and a BCA assay.

**Immobilization of DNA–Aldolase onto Glass Surfaces and Analysis of Activity.** Glass slides (15 mm in diameter) coated with ssDNA (strands A or B) were loaded in a 24 well plate. These slides were incubated with DNA–aldolase conjugate (strand A') for hybridization. PDMS wells were used to form a well on top of the glass slides while in the 24 well plate, and 200  $\mu$ L of 0.025  $\mu$ M conjugate (based on DNA concentration) in 5x SSC + 0.1% Tween 20 was added to the well, just enough to cover the top of the slide. Slides were incubated for 1h in humidifying conditions on an orbital shaker at RT (unless otherwise noted). Following incubation, 2 mL of 5x SSC + 0.1% Tween 20 were added to the wells and the PDMS wells were removed. The glass slides were rinsed in 5x SSC + 0.1% Tween 20 via repeated pipetting and then the plate was shaken twice for 10 min with the wells filled with 2 mL of 1x SSC + 0.1% Tween 20. At this point, the PDMS wells were removed from the glass slides, but the slides remained immersed in solution within the 24 well plate.

After rinsing with SSC, the buffer was exchanged into the activity assay buffer (20 mM potassium phosphate, 10 mM potassium pyrophosphate, 3  $\mu$ M dithiothreitol (DTT) pH 8.5). Each well had NAD<sup>+</sup>, GAPDH, and FBP added to it such that the final concentrations were 1 mM NAD<sup>+</sup>, 1.35  $\mu$ M GAPDH, and 100  $\mu$ M FBP in 500  $\mu$ L total volume. Prior to adding the FBP, the plate was equilibrated to 37 °C. A positive control was also run with the addition of 20 nM DNA–Aldolase conjugate (strand A') in solution with wells containing a glass slide that had the non-complementary DNA strand attached to it. Immediately after the addition of FBP, the absorbance at 340 nm was measured every 5 min for 16 h while holding the temperature at 37 °C (Tecan Infinite 200 Pro plate reader). A standard curve with NADH was also prepared on the same plate, in concentrations ranging from 0 to 100  $\mu$ M. All samples were run in triplicate.

## ■ ASSOCIATED CONTENT

### ● Supporting Information

The Supporting Information is available free of charge on the ACS Publications website at DOI: 10.1021/jacs.6b11716.

Experimental details and supporting figures (PDF)

## ■ AUTHOR INFORMATION

### Corresponding Author

\*mbfrancis@berkeley.edu

### ORCID

Matthew B. Francis: 0000-0003-2837-2538

### Author Contributions

§K.S.P. and T.J.H. contributed equally.

### Notes

The authors declare no competing financial interest.

## ■ ACKNOWLEDGMENTS

The work directed toward N-terminal protein functionalization was funded by NSF (CHE 1413666). The surface immobilization and characterization studies were supported by the U.S. Department of Energy, Office of Science, Office of Basic Energy Sciences, Chemical Sciences, Geosciences, and Biosciences Division under Contract DE-AC02-05CH11231. K.S.P. was supported by a predoctoral fellowship from the NSF and from the Berkeley Chemical Biology Graduate Program (NRSA Training Grant 1 T32 GMO66698).

## ■ REFERENCES

- (1) Witham, C. A.; Huang, W. Y.; Tsung, C. K.; Kuhn, J. N.; Somorjai, G. A.; Toste, F. D. *Nat. Chem.* **2010**, *2*, 36–41.
- (2) Huang, W. Y.; Liu, J. H.-C.; Alayoglu, P.; Li, Y. M.; Witham, C. A.; Tsung, C. K.; Toste, F. D.; Somorjai, G. A. *J. Am. Chem. Soc.* **2010**, *132*, 16771–16773.
- (3) Li, Y.; Liu, J. H.-C.; Witham, C. A.; Huang, W.; Marcus, M. A.; Fakra, S. C.; Alayoglu, P.; Zhu, Z.; Thompson, C. M.; Arjun, A.; Lee, K.; Gross, E.; Toste, F. D.; Somorjai, G. A. *J. Am. Chem. Soc.* **2011**, *133*, 13527–13533.
- (4) Baio, J. E.; Weidner, T.; Baugh, L.; Gamble, L. J.; Stayton, P. S.; Castner, D. G. *Langmuir* **2012**, *28*, 2107–2112.
- (5) Phizicky, E.; Bastiaens, P. I. H.; Zhu, H.; Snyder, M.; Fields, S. *Nature* **2003**, *422*, 208–215.
- (6) Brady, D.; Jordaan, J. *Biotechnol. Lett.* **2009**, *31*, 1639–1650.
- (7) Jonkheijm, P.; Weinrich, D.; Schröder, H.; Niemeyer, C. M.; Waldmann, H. *Angew. Chem., Int. Ed.* **2008**, *47*, 9618–9647.
- (8) Cha, T.; Guo, A.; Zhu, X. *Proteomics* **2005**, *5*, 416–419.
- (9) Vallières, K.; Chevallier, P.; Sarra-Bournet, C.; Turgeon, S.; Laroche, G. *Langmuir* **2007**, *23*, 9745–9751.
- (10) Camarero, J. A.; Kwon, Y.; Coleman, M. A. *J. Am. Chem. Soc.* **2004**, *126*, 14730–14731.
- (11) Buhl, M.; Vonhören, B.; Ravoo, B. J. *Bioconjugate Chem.* **2015**, *26*, 1017–1020.
- (12) Yeritsyan, H. E.; Gasparyan, V. K. *Microchim. Acta* **2012**, *176*, 117–122.
- (13) Taniguchi, K.; Nomura, K.; Hata, Y.; Nishimura, T.; Asami, Y.; Kuroda, A. *Biotechnol. Bioeng.* **2007**, *96*, 1023–1029.
- (14) Kindermann, M.; George, N.; Johnsson, N.; Johnsson, K. *J. Am. Chem. Soc.* **2003**, *125*, 7810–7811.
- (15) Wong, L. S.; Thirlway, J.; Micklefield, J. *J. Am. Chem. Soc.* **2008**, *130*, 12456–12464.
- (16) Abad, J. M.; Mertens, S. F. L.; Pita, M.; Fernandez, V. M.; Schiffrin, D. J. *J. Am. Chem. Soc.* **2005**, *127*, 5689–5694.
- (17) Reynolds, N. P.; Tucker, J. D.; Davison, P. A.; Timney, J. A.; Hunter, C. N.; Leggett, G. J. *J. Am. Chem. Soc.* **2009**, *131*, 896–897.
- (18) Huttsell, S. Q.; Kimple, R. J.; Siderovski, D. P.; Willard, F. S.; Kimple, A. J. *Methods Mol. Biol.* **2010**, *627*, 75–90.
- (19) Nimse, S. B.; Song, K.; Sonawane, M. D.; Sayyed, D. R.; Kim, T. *Sensors* **2014**, *14*, 22208–22229.
- (20) Niemeyer, C. M. *Angew. Chem., Int. Ed.* **2010**, *49*, 1200–1216.
- (21) Beaucage, S. L. *Curr. Med. Chem.* **2001**, *8*, 1213–1244.
- (22) Niemeyer, C. M.; Boldt, L.; Ceyhan, B.; Blohm, D. *Anal. Biochem.* **1999**, *268*, 54–63.
- (23) Bauer, D. M.; Ahmed, I.; Vigovskaya, A.; Fruk, L. *Bioconjugate Chem.* **2013**, *24*, 1094–1101.
- (24) Fruk, L.; Müller, J.; Niemeyer, C. M. *Chem. - Eur. J.* **2006**, *12*, 7448–7457.
- (25) Wold, E. D.; McBride, R.; Axup, J. Y.; Kazane, S. A.; Smider, V. V. *Bioconjugate Chem.* **2015**, *26*, 807–811.
- (26) Behrens, C. R.; Hooker, J. M.; Obermeyer, A. C.; Romanini, D. W.; Katz, E. M.; Francis, M. B. *J. Am. Chem. Soc.* **2011**, *133*, 16398–16401.
- (27) Witus, L. S.; Netirojjanakul, C.; Palla, K. S.; Muehl, E. M.; Weng, C. H.; Iavarone, A. T.; Francis, M. B. *J. Am. Chem. Soc.* **2013**, *135*, 17223–17229.

- (28) Scheck, R. A.; Dedeo, M. T.; Iavarone, A. T.; Francis, M. B. *J. Am. Chem. Soc.* **2008**, *130*, 11762–11770.
- (29) Palla, K. S.; Witus, L. S.; Mackenzie, K. J.; Netirojjanakul, C.; Francis, M. B. *J. Am. Chem. Soc.* **2015**, *137*, 1123–1129.
- (30) Tong, G. J.; Hsiao, S. C.; Carrico, Z. M.; Francis, M. B. *J. Am. Chem. Soc.* **2009**, *131*, 11174–11178.
- (31) Netirojjanakul, C.; Witus, L. S.; Behrens, C. R.; Weng, C.; Iavarone, A. T.; Francis, M. B. *Chem. Sci.* **2013**, *4*, 266–272.
- (32) El Muslemany, L. M.; Twite, A. A.; ElSohly, A. M.; Obermeyer, A. C.; Mathies, R. A.; Francis, M. B. *J. Am. Chem. Soc.* **2014**, *136*, 12600–12606.
- (33) Capehart, S. L.; Coyle, M. P.; Glasgow, J. E.; Francis, M. B. *J. Am. Chem. Soc.* **2013**, *135*, 3011–3016.
- (34) Capehart, S. L.; ElSohly, A. M.; Obermeyer, A. C.; Francis, M. B. *Bioconjugate Chem.* **2014**, *25*, 1888–1892.
- (35) Obermeyer, A. C.; Jarman, J. B.; Netirojjanakul, C.; Francis, M. B. *Angew. Chem., Int. Ed.* **2014**, *53*, 1057–1061.
- (36) Obermeyer, A. C.; Jarman, J. B.; Francis, M. B. *J. Am. Chem. Soc.* **2014**, *136*, 9572–9579.
- (37) Windle, C. L.; Müller, M.; Nelson, A.; Berry, A. *Curr. Opin. Chem. Biol.* **2014**, *19*, 25–33.
- (38) Rosen, C. B.; Kwant, R. L.; MacDonald, J. I.; Rao, M.; Francis, M. B. *Angew. Chem., Int. Ed.* **2016**, *55*, 8585–8588.
- (39) Sasou, M.; Sugiyama, S.; Yoshino, T.; Ohtani, T. *Langmuir* **2003**, *19*, 9845–9849.
- (40) Saha, B.; Saikia, J.; Das, G. *Analyst* **2015**, *140*, 532–542.
- (41) Seeman, N. C. *Annu. Rev. Biochem.* **2010**, *79*, 65–87.
- (42) Phillips, D. C.; York, R. L.; Mermut, O.; McCrea, K. R.; Ward, R. S.; Somorjai, G. A. *J. Phys. Chem. C* **2007**, *111*, 255–261.
- (43) York, R. L.; Browne, W. K.; Geissler, P. L.; Somorjai, G. A. *Isr. J. Chem.* **2007**, *47*, 51–58.